Frontiers in Bioscience Landmark

Front. Biosci. (Landmark Ed) **2026**; 31(5): 46914
https://doi.org/10.31083/FBL46914

Original Research

β-Ecdysterone Attenuates Ang II–Induced Senescence in Human Aortic Smooth Muscle Cells via Autophagy Activation and ROS Suppression Through AKT/mTOR Pathway Inhibition

Di Wu[1,†], Tao Dong[2,†], Yitong Li[1], Honghong Wang[1], Lulu Wang[2], Xiaodong Zhang[2], Chengrun Song[1], Hongming Pan[2], Haifeng Jin[2], Lei Shen[2,*]

[1]Basic Medical Research Center, Qiqihar Medical University, 161006 Qiqihar, Heilongjiang, China
[2]Heilongjiang Provincial Key Laboratory of Medicine-Food Homologous Resources and Metabolic Disease Prevention and Control, Qiqihar Medical University, 161006 Qiqihar, Heilongjiang, China
*Correspondence: qmusl815@126.com (Lei Shen)
[†]These authors contributed equally.

Academic Editor: Amancio Carnero Moya
Submitted: 25 September 2025 Revised: 24 February 2026 Accepted: 4 March 2026 Published: 9 May 2026

Abstract

Background: This study aimed to elucidate the protective effects of β-ecdysterone (β-Ecd) against premature senescence in human aortic smooth muscle cells (HASMCs) and to unravel the underlying mechanisms. **Methods**: HASMCs' senescence was induced with angiotensin II (Ang II), and cells were then treated with β-Ecd. Cell viability was assessed using the Cell Counting Kit-8 (CCK-8) assay. Cellular senescence was evaluated by senescence-associated β-galactosidase (SA-β-gal) staining, cell cycle analysis, and western blotting for the senescence-associated proteins tumor protein p53 (p53) and cyclin-dependent kinase inhibitor 1A (p21). IL-6 and MCP-1 levels in culture supernatants were measured using enzyme-linked immunosorbent assay (ELISA). Autophagy was assessed by microtubule-associated protein 1A/1B light chain 3 (LC3) immunofluorescence, autolysosome staining, and western blotting for LC3 and sequestosome 1 (p62). Intracellular reactive oxygen species (ROS) were quantified by flow cytometry. Transcriptomic profiling using Kyoto Encyclopedia of Genes and Genomes (KEGG), Gene Ontology (GO), and Gene Set Enrichment Analysis (GSEA), along with analyses and molecular docking, was used to explore potential mechanisms, with key findings validated by western blot. **Results**: Ang II induced pronounced senescence in HASMCs, characterized by increased SA-β-gal activity, elevated p53 and p21 expression, G0/G1 cell cycle arrest, impaired autophagic flux, increased ROS accumulation, and elevated secretion of IL-6 and MCP-1. CCK-8 assays confirmed that β-Ecd did not affect HASMCs' viability at concentrations up to 200 µM. Treatment with 200 µM β-Ecd effectively attenuated Ang II–induced senescence, restoring cell cycle distribution, reducing p53 and p21 expression, and suppressing IL-6 and MCP-1 secretion. β-Ecd also enhanced autophagic activity, as evidenced by increased LC3II levels, reduced p62 accumulation, and enhanced autophagosome–lysosome fusion, while significantly decreasing intracellular ROS levels. Inhibition of autophagy with bafilomycin A1 abolished the protective effects of β-Ecd. Transcriptomic and bioinformatics analyses revealed enrichment for pathways related to autophagy regulation, with a prominent role for the PI3K/protein kinase B (AKT)/mechanistic target of rapamycin (mTOR) signaling axis. Consistently, western blot analysis showed that β-Ecd suppressed Ang II–induced phosphorylation of AKT and mTOR. Modulation of AKT activity further supported its involvement in β-Ecd–mediated protection, as AKT inhibition mimicked this effect. In contrast, AKT activation counteracted the pro-autophagic and anti-senescent effects of β-Ecd. Molecular docking further suggested favorable interactions between β-Ecd and AKT isoforms as well as mTOR. **Conclusion**: β-Ecd attenuates Ang II–induced premature senescence in HASMCs by enhancing autophagy and limiting oxidative stress, a process mediated by suppressed AKT/mTOR signaling.

Keywords: ecdysterone; autophagy; reactive oxygen species; cellular senescence

1. Introduction

The global burden of atherosclerotic cardiovascular disease (ASCVD) is increasingly shifting toward younger adults. From 1990 to 2019, the prevalence of ischemic heart disease, ischemic stroke, and peripheral arterial disease among individuals aged 20 to 52 years increased by 20.55%, 11.50%, and 7.38%, respectively [1]. These epidemiological changes suggest a need for a thorough understanding of the molecular mechanisms underlying early-onset vascular aging and for exploring potential preventive strategies. Vascular smooth muscle cells (VSMCs) senescence is recognized as an essential contributor to the initiation and progression of ASCVD. Senescent VSMCs participate in plaque instability, vascular remodeling, and chronic inflammation, thereby contributing to the development of atherosclerosis, hypertension, pulmonary hypertension, and aneurysm formation [2,3]. Previous studies have shown that multiple stress-related processes, including impaired autophagy, oxidative stress, persistent inflammation, and altered calcium signaling, can promote VSMC senescence [4,5]. Accordingly, therapeutic strategies targeting

VSMC senescence may have potential value in reducing cardiovascular risk.

Angiotensin II (Ang II), a key effector peptide of the renin–angiotensin–aldosterone system, plays an essential role in vascular pathophysiology. By promoting excessive production of reactive oxygen species (ROS) and activating NF-κB-dependent inflammatory signaling, Ang II impairs antioxidant defenses, disrupts mitochondrial function, and contributes to premature senescence of vascular cells [6,7]. Increasing evidence from Ang II–induced models of vascular injury indicates that impaired autophagy is closely associated with ROS accumulation and enhanced cell death, thereby aggravating vascular dysfunction [8,9]. In advanced atherosclerosis, deletion of the macrophage-specific autophagy-related gene Atg5 suppresses autophagy, increases oxidative stress, and promotes apoptosis, thereby promoting plaque necrosis [9]. Collectively, these findings indicate that oxidative stress arising from defective autophagy is an essential factor in vascular aging. Given that mTOR and lysosomal signaling pathways are well-recognized regulators of both autophagy and cellular aging, modulation of the PI3K/AKT/mTOR pathway has been proposed as a potential therapeutic strategy for ASCVD [3,4].

Natural products with multitarget properties have attracted increasing interest as potential sources for drug discovery in cardiovascular research. *Achyranthes bidentata* Blume, a traditional East Asian medicinal herb, has long been used to improve circulation and manage vascular disorders [10,11]. Pharmacological studies have shown that its bioactive components exhibit anti-inflammatory, antioxidant, neuroprotective, and anti-atherosclerotic effects [11–13]. Among these components, β-Ecd, also known as 20-hydroxyecdysone, is considered one of the major active phytosterols [14,15]. Previous studies have reported that β-Ecd displays a range of biological activities, including lipid-lowering [16], anti-inflammatory [17], anti-apoptotic [18], neuroprotective [19], antioxidant [20], and autophagy-promoting effects [21]. However, it remains unclear whether β-Ecd can alleviate Ang II-induced VSMC senescence by coordinating autophagy and ROS metabolism. In this study, we investigated the role of β-Ecd in vascular protection and assessed its potential to delay vascular aging and mitigate ASCVD progression.

2. Materials and Methods

2.1 Cell Culture

Human aortic smooth muscle cells (HASMCs; Catalog No. HTX2073P, Otwo Biotech, Shenzhen, China) were cultured in Smooth Muscle Cell Medium (SMCM; Catalog No. 1101, ScienCell, San Diego, CA, USA). Cells were maintained at 37 °C in a humidified incubator with 5% CO_2. HASMCs between passages three and eight were used for all experiments. Cell line identity was validated by short tandem repeat (STR) profiling, and all cultures tested negative for mycoplasma.

2.2 Establishment of Cell Senescence Model and Experimental Groups

Cellular senescence was induced by treating HASMCs with 2 µM Ang II (Catalog No. MB1677, Meilunbio, Dalian, China) for 72 h; this group was designated as the Ang II group . To evaluate the protective effects of β-Ecd, cells were pretreated with 50, 100, or 200 µM β-Ecd (Catalog No. S25531, Yuanye, Shanghai, China) prior to Ang II exposure, designated as the low-, medium-, and high-dose β-Ecd groups, respectively. For mechanistic analyses, cells in the high-dose β-Ecd group were additionally treated with 50 nM bafilomycin A1 (BafA1; Catalog No. HY-100558, MCE, Shanghai, China), 10 µM SC79 (Catalog No. HY-18749, MCE, Shanghai, China), or 2.5 mM N-acetyl-L-cysteine (NAC; Catalog No. A9165, Sigma, Shanghai, China), referred to as the BafA1, SC79, and NAC groups, respectively. In parallel, cells in the Ang II group were treated with 10 µM MK-2206 (Catalog No. GC16304, Glpbio, Shanghai, China) and designated as the MK-2206 group. Untreated HASMCs served as the control group.

2.3 Cell Viability Assay

HASMCs were seeded into 96-well plates and treated with different concentrations of β-Ecd for 72 h. Subsequently, 10 µL of CCK-8 reagent (Catalog No. MA0218-5, MeilunBio, Dalian, China) was added to each well, followed by incubation at 37 °C for 4 h. Absorbance was measured at 450 nm using a microplate reader (SpectraMax iD3; Molecular Devices, USA). Cell viability was analyzed and plotted using GraphPad Prism version 10.1.2 (GraphPad Software LLC, San Diego, CA, USA).

2.4 β-Galactosidase (SA-β-gal) Staining

HASMCs (2.5×10^4 cells/well) were seeded in 24-well plates, pretreated with β-Ecd or BafA1 as described above, and subsequently exposed to Ang II for 72 h. Cells were fixed and stained using a commercial SA-β-gal staining kit (Catalog No. GC16304, Beyotime, Shanghai, China), followed by incubation overnight at 37 °C in a CO_2-free incubator. Senescent cells exhibiting blue staining were observed and quantified using an IX73 inverted microscope (Olympus, Tokyo, Japan).

2.5 Enzyme-Linked Immunosorbent Assay (ELISA)

Cell culture supernatants were collected after treatment with varying concentrations of β-Ecd or Ang II for 72 h to measure IL-6 and MCP-1 levels. ELISA assays were performed according to the manufacturer's instructions (Catalog No. E-EL-H6156, Elabscience, Wuhan, China; Catalog No. E-EL-H6005, Elabscience, Wuhan, China). Absorbance was measured at 450 nm using a SpectraMax iD3 microplate reader (Molecular Devices, USA).

2.6 RNA Sequencing and Bioinformatics

Total RNA was extracted from HASMCs in the Ang II group and the 200 μM β-Ecd group (n = 3 per group) after 72 h of treatment. RNA library preparation and sequencing were conducted on the Illumina NovaSeq X Plus platform (Illumina, San Diego, CA, USA) by Hangzhou Kaitai Biotechnology (Hangzhou, China). Differentially expressed genes (DEGs) were identified using edgeR version 4.0.0 (Bioconductor, http://www.bioconductor.org) with thresholds of $|\log_2$ fold change$| > 1$ and adjusted $p < 0.05$. Volcano plots were generated using ggplot2. Functional enrichment analyses, including Gene Ontology (GO) and Kyoto Encyclopedia of Genes and Genomes (KEGG) pathway analyses, were performed using clusterProfiler ($p < 0.05$). Gene set enrichment analysis (GSEA) was performed using the fgsea package, with |normalized enrichment score| >1 and $p < 0.05$. Data visualization was performed using ggplot2, TBtools-II, and the Bioinformatics platform (https://www.bioinformatics.com.cn).

2.7 Cell Cycle Analysis

HASMCs were treated with 200 μM β-Ecd or 2.5 mM NAC, followed by exposure to 2 μM Ang II for 72 h. Cells were fixed in 70% ethanol overnight at 4 °C, stained with propidium iodide (Catalog No. C1052, Beyotime, Shanghai, China), and analyzed by flow cytometry using a LongCyte C2060 system (Beijing Challen Biotechnology, China).

2.8 Western Blot Analysis

Cells were lysed using RIPA buffer (Catalog No. P0013B, Beyotime, Shanghai, China), and protein concentrations were determined using a BCA assay. Equal amounts of protein were separated by SDS-PAGE and transferred to PVDF membranes (Catalog No. ISEQ00010, Sigma-Aldrich, USA). After blocking, membranes were incubated overnight at 4 °C with primary antibodies against p53 (Catalog No. AP062-1, Beyotime, Shanghai, China), p21 (Catalog No. AP021-1, Beyotime, Shanghai, China), LC3 (Catalog No. 14600-1-AP, Proteintech, Wuhan, China), p62 (Catalog No. 18420-1-AP, Proteintech, Wuhan, China), mTOR (Catalog No. 66888-1-Ig, Proteintech, Wuhan, China), phosphorylated mTOR (p-mTOR; Catalog No. 67778-1-Ig, Proteintech, Wuhan, China), AKT (Catalog No. BM4400, Boster, Wuhan, China), phosphorylated AKT (p-AKT; Catalog No. BM4744, Boster, Wuhan, China), and GAPDH (Catalog No. BM3874, Boster, Wuhan, China), followed by incubation with HRP-conjugated secondary antibodies (Catalog No. AS014, ABclonal, Wuhan, China; Catalog No. AS003, ABclonal, Wuhan, China). Protein bands were visualized using enhanced chemiluminescence (MeilunBio, Dalian, China) and quantified with ImageJ software (NIH, Bethesda, MD, USA).

2.9 ROS Detection

Cells were incubated with 10 μM DCFH-DA (Catalog No. S0033S, Beyotime, Shanghai, China) for 20 min at 37 °C, washed with PBS. Samples were acquired on a BD FACSAria II flow cytometer (BD Biosciences, USA) and analyzed using FlowJo software version 10.8.1 (BD Biosciences, Ashland, OR, USA) to quantify intracellular ROS levels.

2.10 Immunofluorescence Staining

HASMCs cultured on coverslips were fixed with ethanol, permeabilized with Triton X-100, and blocked with goat serum. Cells were incubated overnight at 4 °C with a primary antibody against LC3 (Catalog No. 14600-1-AP, Proteintech, Wuhan, China), followed by incubation with a fluorophore-conjugated an AF647-labeled Goat Anti-Rabbit IgG (H+L) secondary antibody (Catalog No. A0468, Beyotime, Shanghai, China). Nuclei were counterstained, and LC3-positive puncta were visualized using a Revolve fluorescence microscope (Aperbio, Suzhou, China).

2.11 Autophagy-Lysosome Detection

Cells were incubated with DAL Green dye (Catalog No. D675, Dojindo, Japan) for 30 min, followed by treatment with Ang II, β-Ecd, or BafA1 for 6 h. Fluorescence signals were observed using a Revolve confocal imaging system (Aperbio, Suzhou, China).

2.12 Molecular Docking

The three-dimensional structure of β-Ecd was obtained from PubChem and optimized using Chem3D version 22.0 (PerkinElmer Inc., Waltham, MA, USA). Crystal structures of AKT1, AKT2, AKT3, and mTOR were downloaded from the RCSB Protein Data Bank. Molecular docking simulations were performed using AutoDock Vina, and docking poses were visualized with PyMOL. Binding energies lower than –5 kcal/mol were considered indicative of stable interactions. Additional docking validation was conducted using the CB-Dock2 platform (https://cadd.labshare.cn/cb-dock2).

2.13 Statistical Analysis

All experiments were independently repeated at least three times. Data are presented as mean ± standard deviation (SD). Statistical analyses were performed using GraphPad Prism version 10.1.2. Data normality was assessed using the Shapiro–Wilk test. Comparisons among multiple groups were conducted using one-way analysis of variance followed by Tukey's post hoc test. A value of $p < 0.05$ was considered statistically significant.

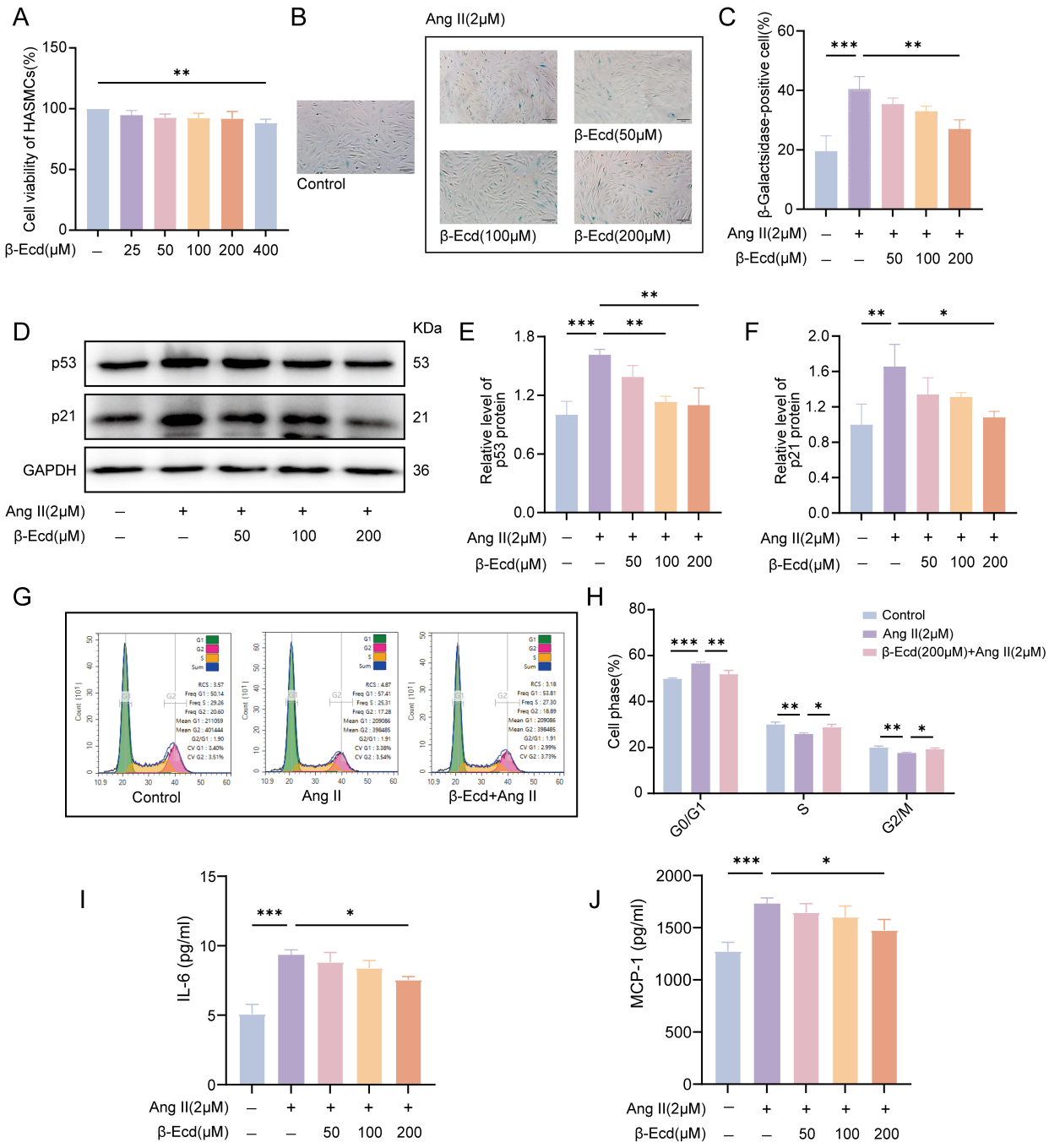

Fig. 1. β-Ecd attenuates Ang II–induced senescence in HASMCs. (A) Effects of β-Ecd on HASMCs viability after 72 h of treatment, as determined by CCK-8 assay. (B) Representative SA-β-gal staining images showing SA-β-gal–positive HASMCs under the indicated treatment conditions. Blue staining indicates SA-β-gal-positive cells. Scale bar = 100 μm. (C) Quantification of SA-β-gal–positive cells (n = 3). (D) Western blot analysis of p53 and p21 protein expression in HASMCs treated with Ang II in the presence or absence of β-Ecd. (E,F) Quantitative analysis of p53 and p21 protein expression normalized to GAPDH (n = 3). (G) Flow cytometric analysis of cell cycle distribution in HASMCs treated with Ang II and/or β-Ecd. (H) Statistical analysis of the proportions of cells in the G0/G1, S, and G2/M phases (n = 3). (I,J) ELISA-based quantification of IL-6 and MCP-1 secretion in HASMCs culture supernatants following Ang II stimulation with or without β-Ecd treatment (n = 3). Values are expressed as mean ± SD. *$p < 0.05$, **$p < 0.01$, ***$p < 0.001$. HASMCs, Human aortic smooth muscle cells; CCK-8, Cell Counting Kit-8; β-Ecd, Ecdysterone; Ang-II, Angiotensin II; SA-β-gal, Senescence-Associated β-Galactosidase; p53, Tumor protein p53; p21, Cyclin-dependent kinase inhibitor 1A; ELISA, Enzyme-linked immunosorbent assay.

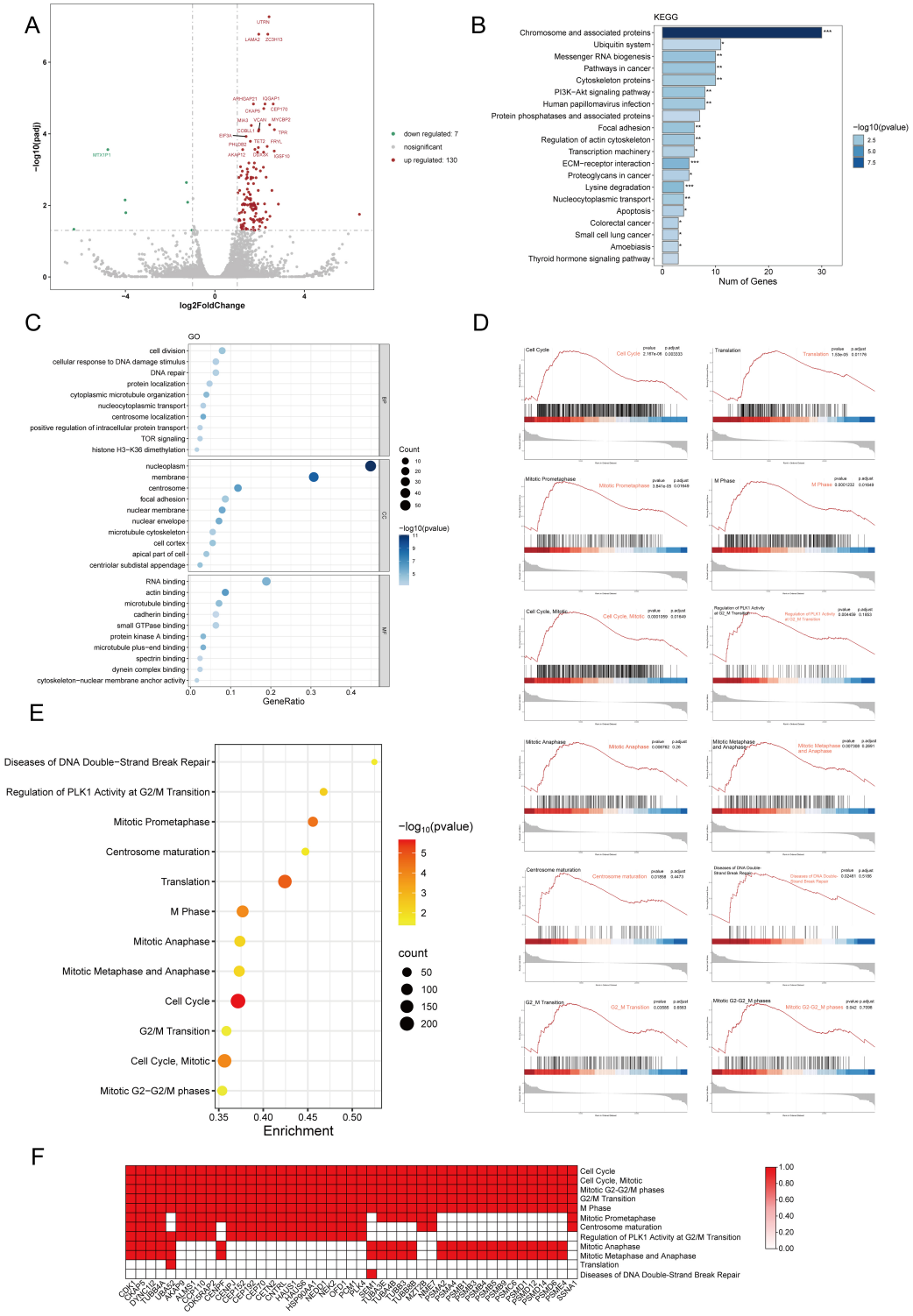

Fig. 2. Transcriptomic changes induced by β-Ecd in senescent HASMCs. (A) Volcano plot of DEGs identified in HASMCs treated with β-Ecd compared with the Ang II group. Red dots indicate upregulated genes, green dots indicate downregulated genes, and gray dots represent genes that did not exhibit significant changes in expression. (B) KEGG pathway enrichment analysis of DEGs. Bar height represents the number of enriched genes, and color intensity reflects the level of statistical significance. $*p < 0.05$, $**p < 0.01$, $***p < 0.001$. (C) GO enrichment analysis of DEGs displayed as a bubble plot. Bubble size corresponds to the number of enriched genes, and bubble color denotes enrichment significance. (D) GSEA of Reactome pathways associated with DEGs. (E) Bubble plot summarizing significantly enriched Reactome pathways identified by GSEA. (F) Heatmap showing enriched Reactome pathways and their associated DEGs. DEGs, Differentially Expressed Genes; KEGG, Kyoto Encyclopedia of Genes and Genomes; GO, Gene Ontology; GSEA, Gene Set Enrichment Analysis.

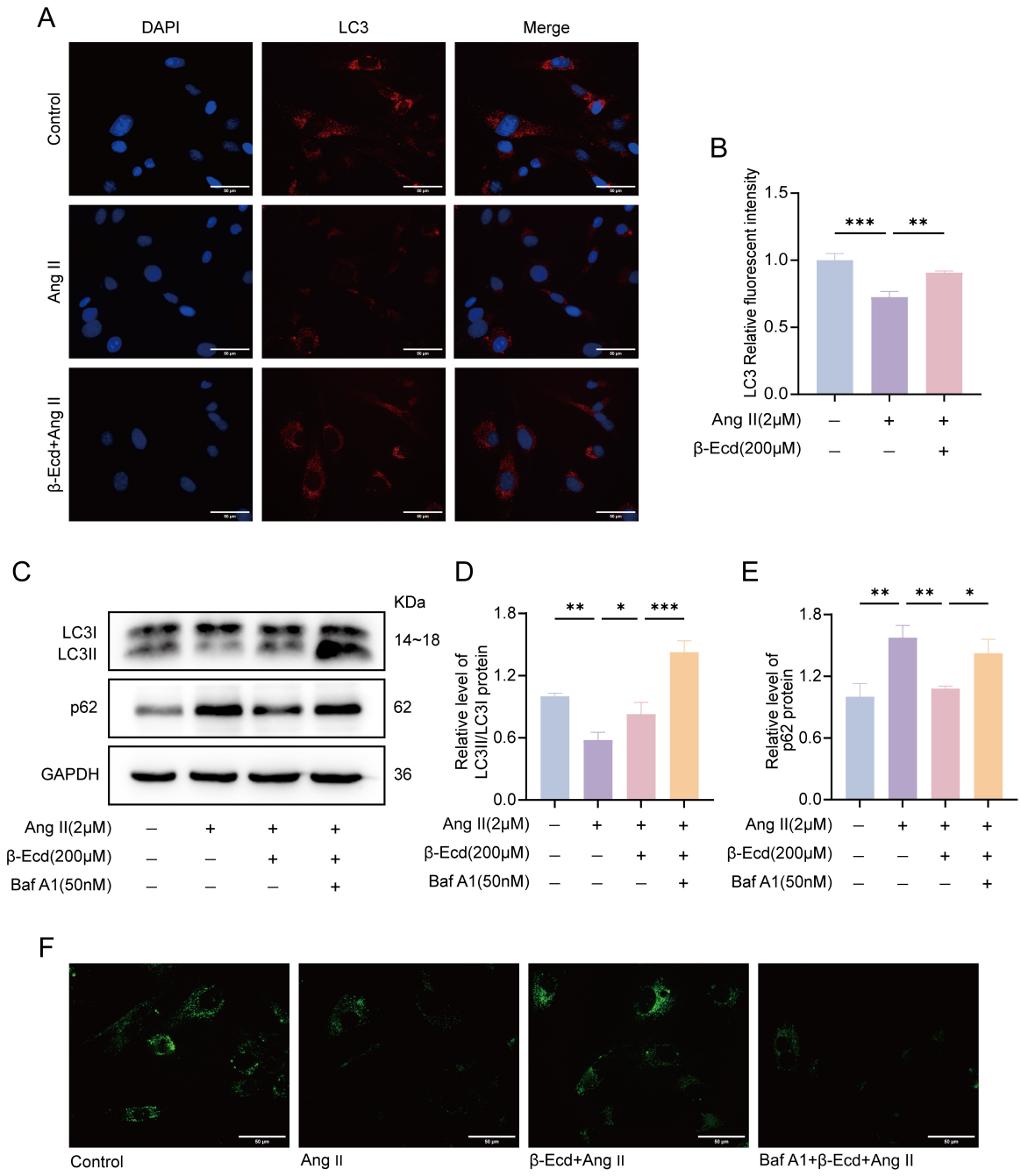

Fig. 3. β-Ecd enhances autophagy activity in HASMCs. (A) Representative immunofluorescence images showing LC3 distribution in HASMCs under the indicated treatment conditions (scale bar = 50 μm). (B) Quantitative analysis of LC3 fluorescence intensity (n = 3). (C) Western blot analysis of the autophagy-related proteins LC3 and p62 in HASMCs. (D,E) Densitometric analysis of LC3 and p62 protein expression levels normalized to GAPDH (n = 3). (F) Autolysosome staining was used to assess autophagic flux in HASMCs under the indicated conditions (scale bar = 50 μm). Values are expressed as mean ± SD. *$p < 0.05$, **$p < 0.01$, ***$p < 0.001$. LC3, Microtubule-associated protein 1A/1B light chain 3; p62, sequestosome 1; Baf A1, Bafilomycin A1.

3. Results

3.1 β-Ecd Attenuates Ang II–Induced HASMCs Senescence

Cell viability assays showed that exposure to β-Ecd at concentrations up to 200 μM for 72 h did not significantly affect HASMCs' viability compared with controls, indicating that β-Ecd within this concentration range was not cytotoxic (Fig. 1A).

To evaluate the effects of β-Ecd on Ang II–induced senescence, HASMCs were pretreated with increasing con-

centrations of β-Ecd and subsequently exposed to Ang II. SA-β-gal staining demonstrated a marked increase in senescent cells following Ang II treatment. Pretreatment with 200 μM β-Ecd significantly reduced the proportion of SA-β-gal-positive HASMCs (Fig. 1B,C). Consistent with these results, Ang II–induced upregulation of p53 and p21 was significantly attenuated by β-Ecd pretreatment, as determined by Western blot analysis (Fig. 1D–F).

Cell cycle analysis further revealed that Ang II induced pronounced G0/G1 phase arrest, accompanied by a reduction in G2/M phase cells. β-Ecd treatment partially reversed Ang II–induced cell cycle arrest, promoting progression into the G2/M phases (Fig. 1G,H). Because cellular senescence is often accompanied by activation of the senescence-associated secretory phenotype (SASP), we next assessed inflammatory cytokine secretion. ELISA analysis showed that Ang II increased IL-6 and MCP-1 secretion in HASMCs, whereas 200 μM β-Ecd significantly inhibited this response (Fig. 1I,J). Overall, these results indicate that β-Ecd mitigates Ang II–induced HASMC senescence, as evidenced by normalization of the cell cycle distribution and reduced SASP factor production.

3.2 Transcriptomic Profiling of β-Ecd–Treated HASMCs

RNA sequencing analysis revealed 137 DEGs between the β-Ecd–treated group and the Ang II groups, of which 130 were upregulated and 7 downregulated (Fig. 2A; **Supplementary Table 1**). KEGG pathway enrichment analysis revealed 18 significantly enriched pathways, with the PI3K–AKT signaling pathway among the most prominently represented (Fig. 2B). GO enrichment analysis indicated that the DEGs were significantly enriched in terms related to cytoplasmic microtubule organization, TOR signaling, protein kinase A binding, and small GTPase binding (Fig. 2C).

GSEA identified 99 enriched Reactome pathways (**Supplementary Table 2**), among which 12 were positively enriched. These pathways were mainly involved in cell cycle regulation, PLK1-mediated signaling, G2/M phase transition, DNA repair, centrosome maturation, and mitotic progression (Fig. 2D,E). Heatmap visualization further highlighted 47 DEGs with relatively high normalized expression, including CDK1, NEK2, HSP90AA1, and CENPF, which are involved in mitotic control and cell proliferation (Fig. 2F). Taken together, these results indicate that β-Ecd treatment is associated with changes in gene expression related to cell cycle progression and proliferation, potentially relevant to Ang II–induced senescence.

3.3 β-Ecd Promotes Autophagy and Reduces ROS Accumulation

Immunofluorescence analysis showed that LC3 puncta were significantly reduced in Ang II–treated HASMCs compared with control cells. This reduction was partially inhibited following β-Ecd treatment (Fig. 3A,B). Consistent with these observations, Western blot analysis demonstrated that Ang II treatment decreased the LC3II/LC3I ratio and increased p62 protein levels, whereas β-Ecd treatment attenuated these changes. The addition of the autophagy inhibitor BafA1 abolished the effects of β-Ecd, resulting in LC3II accumulation and increased p62 levels (Fig. 3C–E). Autophagic flux analysis showed that Ang II reduced autolysosome formation, while β-Ecd significantly enhanced it. In contrast, BafA1 treatment markedly reduced autolysosome formation in Ang II + β-Ecd–treated cells (Fig. 3F).

ROS measurements revealed that Ang II significantly increased intracellular ROS levels. Treatment with NAC inhibited ROS generation, while β-Ecd produced a similar suppressive effect. In contrast, BafA1 attenuated the antioxidant effect of β-Ecd (Fig. 4A–D). Consistent with these findings, SA-β-gal staining demonstrated that β-Ecd treatment reduced Ang II-induced cellular senescence, whereas BafA1 restored senescence levels (Fig. 4E,F). Similarly, β-Ecd decreased Ang II–induced upregulation of p53 and p21, while BafA1 partially counteracted this effect (Fig. 4G–I). Overall, these findings indicate that the anti-senescent effects of β-Ecd in HASMCs are closely associated with enhanced autophagic activity and reduced ROS accumulation.

3.4 β-Ecd Attenuates Ang II–Induced Activation of AKT/mTOR Signaling

Western blot analysis showed that Ang II treatment significantly increased the ratios of p-AKT/AKT and p-mTOR/mTOR compared with control cells. Pretreatment with β-Ecd markedly reduced both p-AKT/AKT and p-mTOR/mTOR ratios, suggesting reduced activation of AKT/mTOR signaling (Fig. 5A–C). In addition, compared with the Ang II group, treatment with the AKT inhibitor MK-2206 significantly decreased the levels of p-AKT/AKT, p-mTOR/mTOR, as well as the senescence-associated proteins p53 and p21 (Fig. 5D–I). Conversely, treatment with the AKT activator SC79 largely inhibited the effects of β-Ecd, restoring AKT and mTOR phosphorylation and the expression of p53 and p21 (Fig. 5D–I). These results further support the involvement of the AKT/mTOR pathway in the anti-senescence effect of β-Ecd on HASMCs.

Molecular docking analysis suggested potential interactions between β-Ecd and components of the AKT/mTOR pathway. β-Ecd showed favorable predicted binding energies with AKT1, AKT2, AKT3, and mTOR (–8.0, –8.5, –8.7, and –8.6 kcal/mol, respectively) and formed multiple hydrogen bonds. Specifically, β-Ecd formed hydrogen bonds with ARG328, TYR38, and LYS30 on AKT1; VAL272, TYR327, ASP324, and LEU52 on AKT2; GLU154, GLN44, GLN38, and GLU109 on AKT3; and GLU95, GLN140, ASP322, and ARG227 on mTOR (Fig. 6A–D). These interactions were further supported by CB-Dock2 analysis, which yielded comparable or slightly

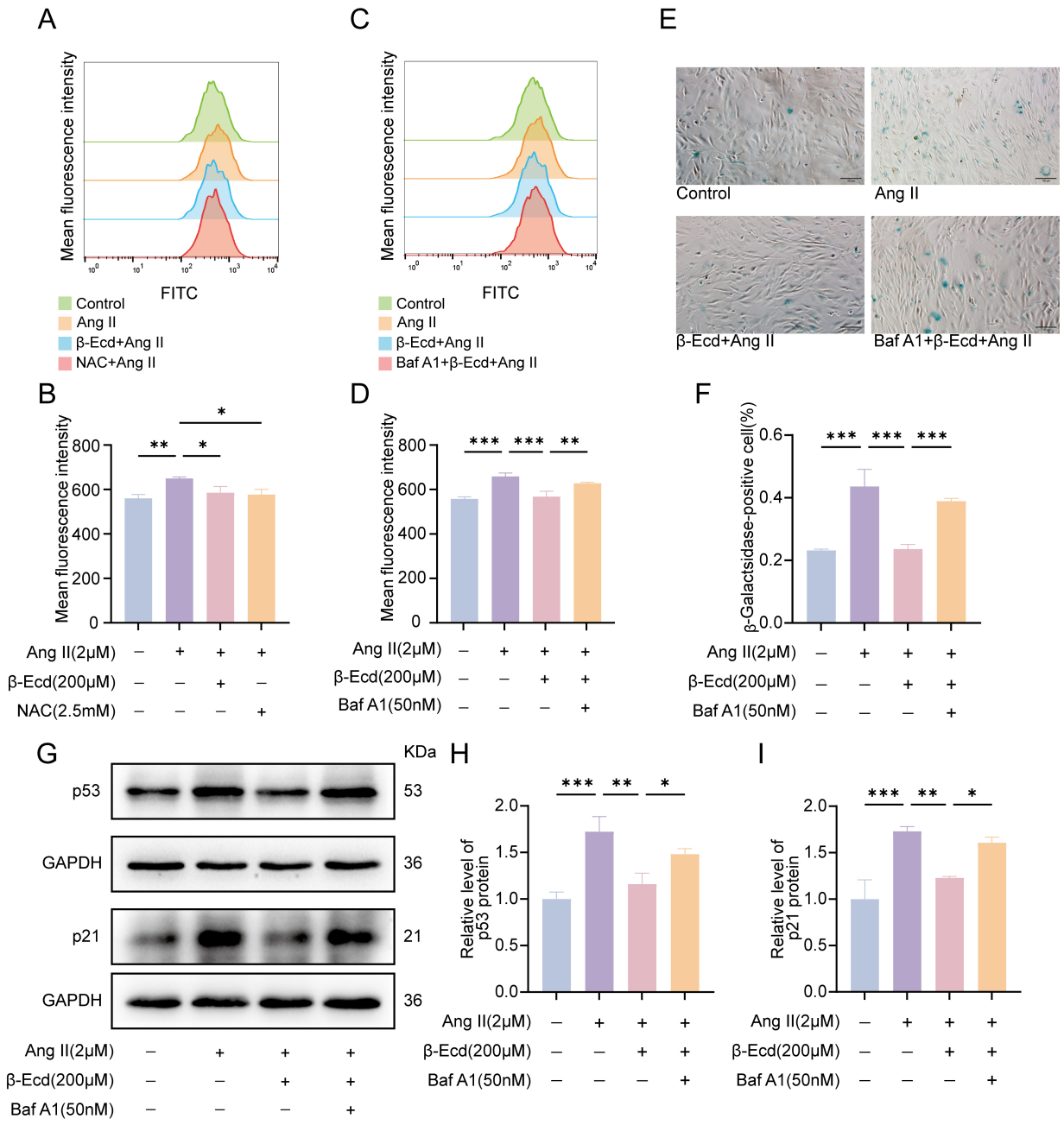

Fig. 4. Autophagy-associated regulation of oxidative stress and senescence by β-Ecd in HASMCs. (A) Representative flow cytometry plots showing intracellular ROS levels in HASMCs following the indicated treatments. (B) Quantification of intracellular ROS levels in each group (n = 3). (C) Flow cytometric analysis of ROS levels following combined β-Ecd and BafA1 treatment. (D) Quantitative comparison of ROS levels in HASMCs (n = 3). (E) Representative SA-β-gal staining images used to evaluate cellular senescence in HASMCs (scale bar = 100 μm). (F) Quantification of SA-β-gal–positive cells (n = 3). (G) Western blot analysis of the senescence-associated proteins p53 and p21 in HASMCs. (H,I) Quantitative analysis of p53 and p21 protein expression levels normalized to GAPDH (n = 3). Values are expressed as mean ± SD. *$p < 0.05$, **$p < 0.01$, ***$p < 0.001$. NAC, N-acetyl-L-cysteine.

stronger predicted binding energies (–8.2 to –9.4 kcal/mol; Fig. 6E–H). Taken together, these results indicate that β-Ecd attenuates Ang II–induced HASMC senescence, associated with reduced AKT/mTOR signaling activity, which may involve interactions with components of this pathway.

4. Discussion

Substantial evidence indicates that VSMCs within atherosclerotic plaques exhibit reduced proliferative capacity and gradually acquire features of cellular senescence, which contributes to plaque instability and disease progres-

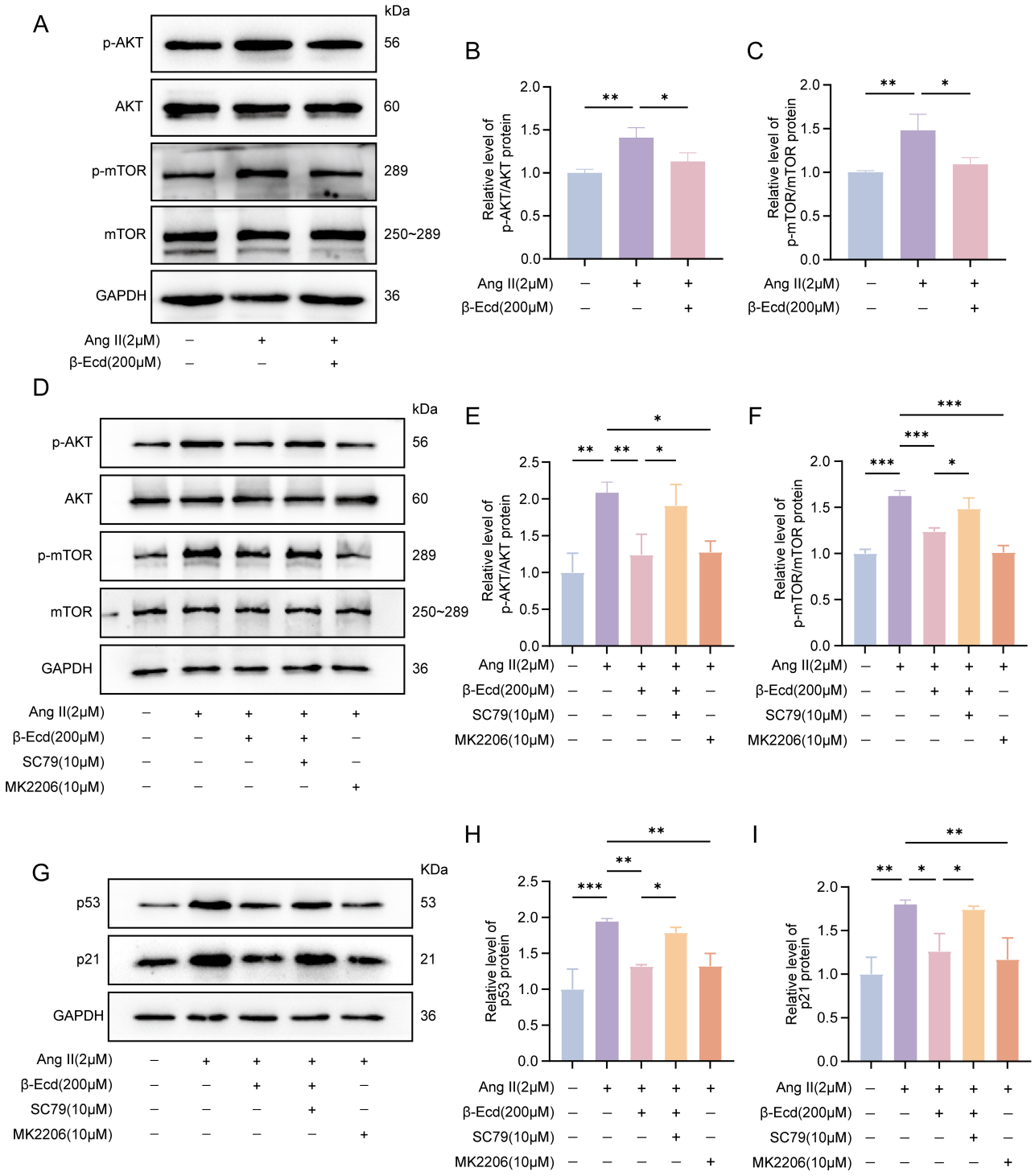

Fig. 5. β-Ecd attenuates Ang II–induced activation of the AKT/mTOR signaling pathway in HASMCs. (A) Representative Western blot images showing total and phosphorylated AKT and mTOR protein levels in HASMCs under the indicated treatment conditions. (B,C) Quantitative analysis of the p-AKT/AKT and p-mTOR/mTOR ratios in each group (n = 3). (D) Representative Western blot images showing p-AKT, AKT, p-mTOR, mTOR, p53, and p21 expression in HASMCs following modulation of AKT signaling with MK-2206 or SC79. (E,F) Quantitative analysis of p-AKT/AKT and p-mTOR/mTOR ratios (n = 3). (G–I) Quantification of p53 and p21 protein expression levels normalized to GAPDH (n = 3). Data are presented as mean ± SD. *$p < 0.05$, **$p < 0.01$, ***$p < 0.001$. AKT, Protein Kinase B; p-AKT, Phosphorylated AKT; mTOR, Mechanistic Target of Rapamycin; p-mTOR, Phosphorylated mTOR.

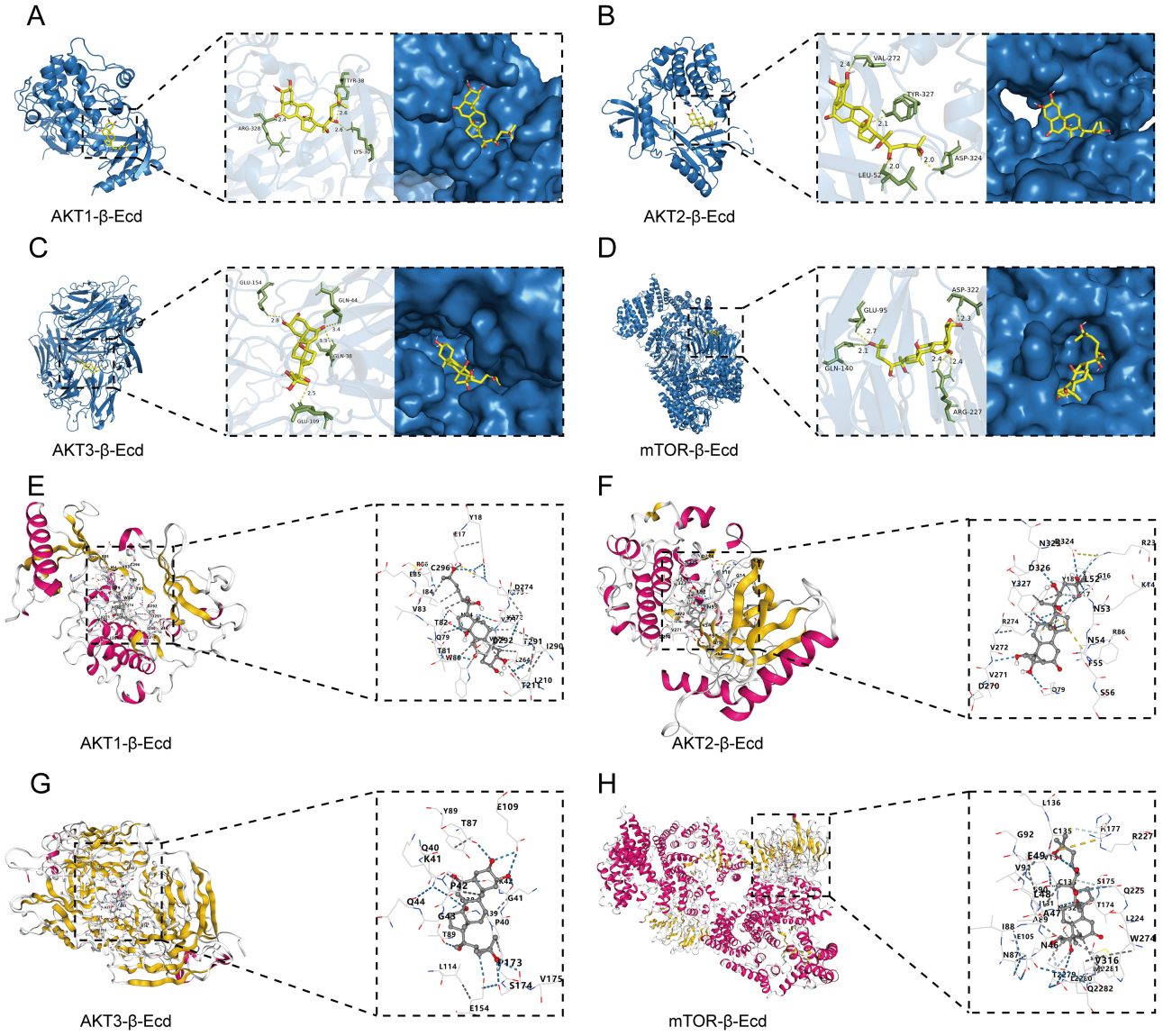

Fig. 6. Molecular docking analysis of β-Ecd with components of the AKT/mTOR signaling pathway. (A–D) Predicted binding modes of β-Ecd with AKT1, AKT2, AKT3, and mTOR, as determined by AutoDock Vina and visualized using PyMOL. (E–H) Independent docking analysis of β-Ecd with AKT1, AKT2, AKT3, and mTOR was performed using the CB-Dock2 platform.

sion [22]. Previous studies have shown that β-Ecd can restore impaired autophagy in a tert-butyl hydroperoxide-induced apoptosis model of rat nucleus pulposus cells [21] and, when combined with paeoniflorin, exerts protective effects against oxidative stress and ferroptosis in a model of cardiac hypertrophy [20]. However, the role of β-Ecd in regulating premature senescence in HASMCs remains unclear. In this study, we show that β-Ecd attenuates Ang II–induced senescence in HASMCs and reduces intracellular ROS accumulation. These effects are accompanied by enhanced autophagic activity and suppression of AKT/mTOR signaling, suggesting a mechanistic link between β-Ecd–mediated autophagy regulation and the alleviation of cellular senescence.

SA-β-gal activity and the upregulation of p53 and p21 are widely recognized markers of cellular senescence, with cell cycle arrest representing another key hallmark [23,24]. In the present study, Ang II treatment markedly increased SA-β-gal positivity, elevated p53 and p21 expression, and induced G0/G1 phase arrest in HASMCs. Notably, treatment with 200 μM β-Ecd effectively attenuated these senescence-associated alterations. In addition to these cell-intrinsic senescence markers, senescent VSMCs actively influence the vascular microenvironment through the SASP, characterized by increased secretion of pro-inflammatory cytokines and chemokines. In line with this, our results showed that Ang II treatment enhanced the secretion of the SASP factors IL-6 and MCP-1, whereas β-Ecd significantly suppressed their production.

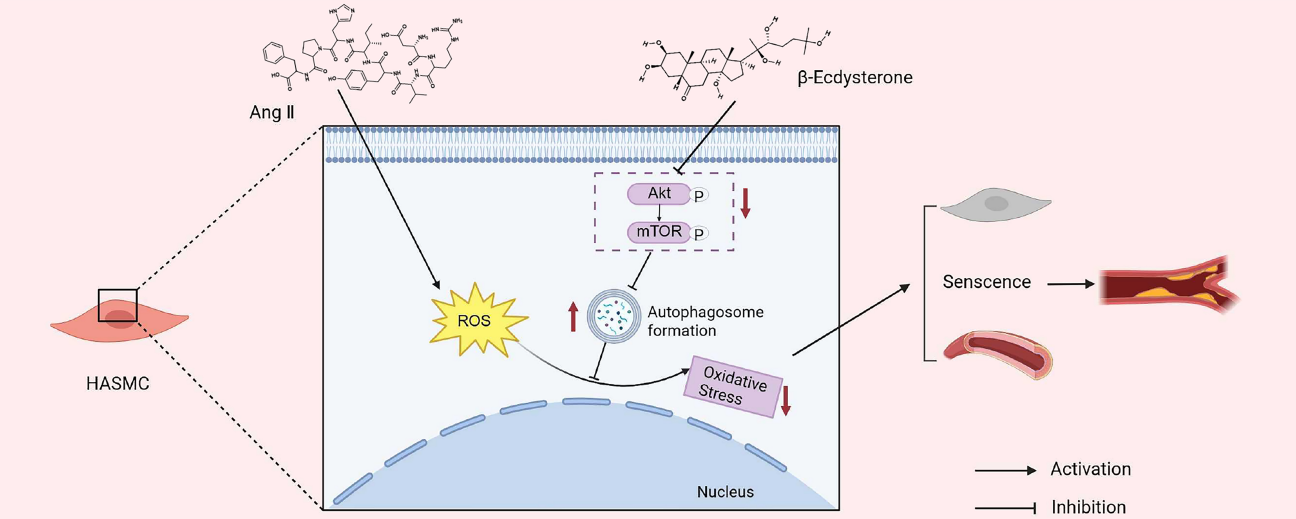

Fig. 7. Proposed mechanism by which β-Ecd delays HASMCs senescence. β-Ecd enhances autophagic activity and promotes autophagosome–lysosome fusion in HASMCs, thereby reducing intracellular oxidative stress and improving cellular homeostasis. These effects collectively alleviate Ang II–induced premature senescence in HASMCs. The autophagy-regulating action of β-Ecd appears to be mediated, at least in part, through inhibition of the AKT/mTOR signaling pathway. Created with BioRender.com.

These results suggest that β-Ecd not only alleviates intrinsic senescence-related alterations in HASMCs but may also attenuate the pro-inflammatory paracrine effects of senescent cells, which are implicated in vascular inflammation and plaque progression.

Autophagy is a fundamental cellular process that maintains protein and organelle homeostasis and contributes to the regulation of cellular senescence. When this process is impaired, damaged proteins and organelles accumulate, oxidative stress increases, and VSMC senescence and atherosclerosis progression are consequently accelerated [22,25]. LC3II, which localizes to autophagosome membranes, is commonly used as a marker of autophagosome formation [26], whereas p62 accumulation reflects defective autophagic degradation [27]. It has been reported that elevated autophagy can inhibit Ang IIinduced senescence in VSMCs [28]. Our data indicate that Ang II treatment reduced the LC3II/LC3I ratio and increased p62 expression. In contrast, β-Ecd treatment restored LC3II levels and reduced p62 accumulation. Moreover, pharmacological inhibition of autophagy with BafA1, which blocks autophagosome–lysosome fusion [29], partially attenuated the protective effects of β-Ecd, supporting the involvement of autophagy activation in its anti-senescent action.

In our Ang II–treated HASMC model, increases in ROS were closely associated with defective autophagy and the development of a senescent phenotype. Ang II markedly elevated intracellular ROS and, concurrently, impaired autophagic flux, as indicated by a reduced LC3II/LC3I ratio, p62 accumulation, and decreased autolysosome formation. These changes occurred alongside increased SA-β-gal positivity, upregulation of p53 and p21, G0/G1 arrest, and elevated secretion of IL-6 and MCP-1. Treatment with β-Ecd improved autophagic flux, reduced ROS levels, and attenuated the secretion of senescence markers and SASP factors. Prior work has linked oxidative stress to the establishment and maintenance of stress-induced senescence through metabolic disruption, mitochondrial injury, and persistent DNA damage signaling [30,31], and ROS scavenging has been reported to blunt Ang II–driven senescence phenotypes [32]. Importantly, blockade of autophagosome-lysosome fusion with BafA1 largely abolished the ROS-lowering and anti-senescent effects of β-Ecd, demonstrating that an intact autophagic process is essential for β-Ecd–mediated protection. Together, our data suggest that β-Ecd lowers ROS primarily by enhancing autophagic function. Although we did not directly assess mitochondrial function, previous study has established a close association between mitophagy, ROS, and cellular senescence. Impairment of mitophagy results in excessive mitochondrial aggregation, leading to increased intracellular ROS accumulation and accelerated cellular senescence [33]. Future studies will examine mitophagy to clarify the contribution of mitochondrial dysfunction to the senescence program and to determine how β-Ecd modulates this process.

The PI3K/AKT/mTOR pathway is a central regulator of autophagy and cellular senescence and has been implicated in the progression of atherosclerosis [34,35]. In addition, modulation of PI3K/AKT/mTOR signaling through P2RY12 receptor activation [36] or Sirtuin 3 [37] has been reported to influence senescence and oxidative stress by regulating autophagy. In this study, AngII treatment enhanced the phosphorylation of AKT and mTOR in HASMCs. This activation was significantly inhibited by β-Ecd, an effect similar to that of MK-2206. Con-

versely, SC79 attenuated the inhibitory effects of β-Ecd on the AKT/mTOR signaling pathway and senescence-associated markers, providing functional evidence that the AKT/mTOR pathway is involved in the protective effects of β-Ecd. Furthermore, molecular docking suggested potential binding of β-Ecd to AKT isoforms and mTOR, supporting a plausible molecular basis for pathway modulation.

In summary, our findings demonstrate that β-Ecd attenuates Ang II–induced premature senescence in HASMCs by restoring autophagic flux, reducing oxidative stress, and suppressing AKT/mTOR signaling (Fig. 7). Given the critical role of VSMC senescence in atherosclerosis pathogenesis, this study provides mechanistic insight into the vascular protective effects of β-Ecd and suggests that it may be relevant to strategies targeting vascular aging and atherosclerotic disease progression.

5. Limitations

Several limitations of this study should be noted. First, although pharmacological approaches were used to modulate AKT signaling, the inclusion of genetic strategies, such as siRNA-mediated knockdown or overexpression of key pathway components, would provide more substantial evidence of causal involvement. Second, the present findings are based on *in vitro* HASMC models; validation in *in vivo* atherosclerosis models will be necessary to assess their translational relevance. Thirdly, while molecular docking analyses serve as a preliminary indication of potential direct interactions between β-Ecd and the AKT/mTOR pathway, definitive identification of key functional binding sites will require future studies using site-directed mutagenesis or genetic silencing.

6. Conclusion

β-Ecd attenuates Ang II–induced senescence in HASMCs by enhancing autophagic activity and limiting intracellular ROS accumulation, effects that are associated with suppression of the AKT/mTOR signaling pathway. These findings suggest that β-Ecd may have the potential to modulate vascular senescence and maintain vascular homeostasis, while providing mechanistic insight into strategies to target vascular aging–related cardiovascular diseases.

Availability of Data and Materials

The data used to support the findings of the present study are included within the article. The dataset used during the current study is available from the corresponding author upon reasonable request.

Author Contributions

LS, HJ and HP designed the research study. DW, YL, HW and LW performed the research. DW, TD, XZ and CS analyzed the data and interpretation. LS, DW and TD wrote the manuscript. All authors contributed to editorial changes in the manuscript. All authors have read and approve the final manuscript. All authors have participated sufficiently in the work and agreed to be accountable for all aspects of the work.

Ethics Approval and Consent to Participate

Not applicable.

Acknowledgment

Not applicable.

Funding

This project was supported by research funds from the Qiqihar Municipal Science and Technology Bureau Joint Guidance Project (LSFGG-2025128), Postgraduate Innovation Fund Project of Qiqihar Medical College in 2024 (QYYCX2024-24), Engineering Research Center of Natural Cosmeceuticals College of Fujian Province Fund (XMMC-OP2024008), Construction Project of Dominant Characteristic Disciplines of Qiqihar Medical University (QYZDXK-013, Human Anatomy and Histoembryology).

Conflict of Interest

The authors declare no conflict of interest.

Supplementary Material

Supplementary material associated with this article can be found, in the online version, at https://doi.org/10.31083/FBL46914.

References

[1] Li Z, Yang Y, Wang X, Yang N, He L, Wang J, *et al*. Comparative analysis of atherosclerotic cardiovascular disease burden between ages 20-54 and over 55 years: insights from the Global Burden of Disease Study 2019. BMC Medicine. 2024; 22: 303. https://doi.org/10.1186/s12916-024-03527-4.

[2] Lin MJ, Hu SL, Tian Y, Zhang J, Liang N, Sun R, *et al*. Targeting Vascular Smooth Muscle Cell Senescence: A Novel Strategy for Vascular Diseases. Journal of Cardiovascular Translational Research. 2023; 16: 1010–1020. https://doi.org/10.1007/s12265-023-10377-7.

[3] Suda M, Paul KH, Minamino T, Miller JD, Lerman A, Ellison-Hughes GM, *et al*. Senescent Cells: A Therapeutic Target in Cardiovascular Diseases. Cells. 2023; 12: 1296. https://doi.org/10.3390/cells12091296.

[4] Shu Z, Li X, Zhang W, Huyan Z, Cheng D, Xie S, *et al*. MG-132 activates sodium palmitate-induced autophagy in human vascular smooth muscle cells and inhibits senescence via the PI3K/AKT/mTOR axis. Lipids in Health and Disease. 2024; 23: 282. https://doi.org/10.1186/s12944-024-02268-w.

[5] Li X, Chen M, Chen X, He X, Li X, Wei H, *et al*. TRAP1 drives smooth muscle cell senescence and promotes atherosclerosis via HDAC3-primed histone H4 lysine 12 lactylation. European Heart Journal. 2024; 45: 4219–4235. https://doi.org/10.1093/eurheartj/ehae379.

[6] Whaley-Connell A, Johnson MS, Sowers JR. Aldosterone: role in the cardiometabolic syndrome and resistant hypertension.

Progress in Cardiovascular Diseases. 2010; 52: 401–409. https://doi.org/10.1016/j.pcad.2009.12.004.

[7] Kunieda T, Minamino T, Nishi JI, Tateno K, Oyama T, Katsuno T, *et al*. Angiotensin II induces premature senescence of vascular smooth muscle cells and accelerates the development of atherosclerosis via a p21-dependent pathway. Circulation. 2006; 114: 953–960. https://doi.org/10.1161/CIRCULATIONAHA.106.626606.

[8] Li C, Lin L, Zhang L, Xu R, Chen X, Ji J, *et al*. Long noncoding RNA p21 enhances autophagy to alleviate endothelial progenitor cells damage and promote endothelial repair in hypertension through SESN2/AMPK/TSC2 pathway. Pharmacological Research. 2021; 173: 105920. https://doi.org/10.1016/j.phrs.2021.105920.

[9] Liao X, Sluimer JC, Wang Y, Subramanian M, Brown K, Pattison JS, *et al*. Macrophage autophagy plays a protective role in advanced atherosclerosis. Cell Metabolism. 2012; 15: 545–553. https://doi.org/10.1016/j.cmet.2012.01.022.

[10] Hyun SW, Lee TG, Song SJ, Kim CS. Evaluation of oral toxicity and genotoxicity of Achyranthis Radix extract. Journal of Ethnopharmacology. 2021; 274: 113944. https://doi.org/10.1016/j.jep.2021.113944.

[11] Chen YR, Niu YS, Zhou HL. Achyranthes bidentata Blume (Amaranthaceae): a review of its botany, traditional uses, phytochemistry, pharmacology, and toxicology. The Journal of Pharmacy and Pharmacology. 2024; 76: 930–966. https://doi.org/10.1093/jpp/rgae012.

[12] He X, Wang X, Fang J, Chang Y, Ning N, Guo H, *et al*. The genus Achyranthes: A review on traditional uses, phytochemistry, and pharmacological activities. Journal of Ethnopharmacology. 2017; 203: 260–278. https://doi.org/10.1016/j.jep.2017.03.035.

[13] Mohammed SAD, Liu H, Baldi S, Chen P, Lu F, Liu S. GJD Modulates Cardiac/Vascular Inflammation and Decreases Blood Pressure in Hypertensive Rats. Mediators of Inflammation. 2022; 2022: 7345116. https://doi.org/10.1155/2022/7345116.

[14] Zou Y, Wang R, Guo H, Dong M. Phytoestrogen β-Ecdysterone Protects PC12 Cells Against MPP+-Induced Neurotoxicity In Vitro: Involvement of PI3K-Nrf2-Regulated Pathway. Toxicological Sciences: an official journal of the Society of Toxicology. 2015; 147: 28–38. https://doi.org/10.1093/toxsci/kfv111.

[15] Xu T, Niu C, Zhang X, Dong M. β-Ecdysterone protects SH-SY5Y cells against β-amyloid-induced apoptosis via c-Jun N-terminal kinase- and Akt-associated complementary pathways. Laboratory Investigation. 2018; 98: 489–499. https://doi.org/10.1038/s41374-017-0009-0.

[16] Buniam J, Chukijrungroat N, Rattanavichit Y, Surapongchai J, Weerachayaphorn J, Bupha-Intr T, *et al*. 20-Hydroxyecdysone ameliorates metabolic and cardiovascular dysfunction in high-fat-high-fructose-fed ovariectomized rats. BMC Complementary Medicine and Therapies. 2020; 20: 140. https://doi.org/10.1186/s12906-020-02936-1.

[17] Zhang X, Xu X, Xu T, Qin S. β-Ecdysterone suppresses interleukin-1β-induced apoptosis and inflammation in rat chondrocytes via inhibition of NF-κB signaling pathway. Drug Development Research. 2014; 75: 195–201. https://doi.org/10.1002/ddr.21170.

[18] Pan Z, Niu Y, Liang Y, Zhang X, Dong M. β-Ecdysterone Protects SH-SY5Y Cells Against 6-Hydroxydopamine-Induced Apoptosis via Mitochondria-Dependent Mechanism: Involvement of p38(MAPK)-p53 Signaling Pathway. Neurotoxicity Research. 2016; 30: 453–466. https://doi.org/10.1007/s12640-016-9631-7.

[19] Liu H, Yu C, Xu T, Zhang X, Dong M. Synergistic protective effect of paeoniflorin and β-ecdysterone against rotenone-induced neurotoxicity in PC12 cells. Apoptosis. 2016; 21: 1354–1365. https://doi.org/10.1007/s10495-016-1293-7.

[20] Yan P, Li X, He Y, Zhang Y, Wang Y, Liu J, *et al*. The synergistic protective effects of paeoniflorin and β-ecdysterone against cardiac hypertrophy through suppressing oxidative stress and ferroptosis. Cellular Signalling. 2025; 125: 111509. https://doi.org/10.1016/j.cellsig.2024.111509.

[21] Wen F, Yu J, He CJ, Zhang ZW, Yang AF. β ecdysterone protects against apoptosis by promoting autophagy in nucleus pulposus cells and ameliorates disc degeneration. Molecular Medicine Reports. 2019; 19: 2440–2448. https://doi.org/10.3892/mmr.2019.9861.

[22] Grootaert MOJ, Moulis M, Roth L, Martinet W, Vindis C, Bennett MR, *et al*. Vascular smooth muscle cell death, autophagy and senescence in atherosclerosis. Cardiovascular Research. 2018; 114: 622–634. https://doi.org/10.1093/cvr/cvy007.

[23] Bernard M, Yang B, Migneault F, Turgeon J, Dieudé M, Olivier MA, *et al*. Autophagy drives fibroblast senescence through MTORC2 regulation. Autophagy. 2020; 16: 2004–2016. https://doi.org/10.1080/15548627.2020.1713640.

[24] Sikora E, Bielak-Zmijewska A, Mosieniak G. A common signature of cellular senescence; does it exist? Ageing Research Reviews. 2021; 71: 101458. https://doi.org/10.1016/j.arr.2021.101458.

[25] Wirawan E, Vanden Berghe T, Lippens S, Agostinis P, Vandenabeele P. Autophagy: for better or for worse. Cell Research. 2012; 22: 43–61. https://doi.org/10.1038/cr.2011.152.

[26] Mondaca-Ruff D, Quiroga C, Norambuena-Soto I, Riquelme JA, San Martin A, Bustamante M, *et al*. Regulation of total LC3 levels by angiotensin II in vascular smooth muscle cells. Journal of Cellular and Molecular Medicine. 2022; 26: 1710–1713. https://doi.org/10.1111/jcmm.17215.

[27] Mizushima N, Komatsu M. Autophagy: renovation of cells and tissues. Cell. 2011; 147: 728–741. https://doi.org/10.1016/j.cell.2011.10.026.

[28] Xu XJ, Zhao WB, Feng SB, Sun C, Chen Q, Ni B, *et al*. Celastrol alleviates angiotensin II mediated vascular smooth muscle cell senescence via induction of autophagy. Molecular Medicine Reports. 2017; 16: 7657–7664. https://doi.org/10.3892/mmr.2017.7533.

[29] Wang X, Zhang M, Mao C, Zhang C, Ma W, Tang J, *et al*. Icariin alleviates ferroptosis-related atherosclerosis by promoting autophagy in xo-LDL-induced vascular endothelial cell injury and atherosclerotic mice. Phytotherapy Research. 2023; 37: 3951–3963. https://doi.org/10.1002/ptr.7854.

[30] Zhang Y, Peng X, Xue M, Liu J, Shang G, Jiang M, *et al*. SARS-COV-2 spike protein promotes RPE cell senescence via the ROS/P53/P21 pathway. Biogerontology. 2023; 24: 813–827. https://doi.org/10.1007/s10522-023-10019-0.

[31] Davalli P, Mitic T, Caporali A, Lauriola A, D'Arca D. ROS, Cell Senescence, and Novel Molecular Mechanisms in Aging and Age-Related Diseases. Oxidative Medicine and Cellular Longevity. 2016; 2016: 3565127. https://doi.org/10.1155/2016/3565127.

[32] Tsai IC, Pan ZC, Cheng HP, Liu CH, Lin BT, Jiang MJ. Reactive oxygen species derived from NADPH oxidase 1 and mitochondria mediate angiotensin II-induced smooth muscle cell senescence. Journal of Molecular and Cellular Cardiology. 2016; 98: 18–27. https://doi.org/10.1016/j.yjmcc.2016.07.001.

[33] Qu X, Pan P, Cao S, Ma Y, Yang J, Gao H, *et al*. *Immp2l* Deficiency Induced Granulosa Cell Senescence Through STAT1/ATF4 Mediated UPR^{mt} and STAT1/(ATF4)/HIF1α/BNIP3 Mediated Mitophagy: Prevented by Enocyanin. International Journal of Molecular Sciences. 2024; 25: 11122. https://doi.org/10.3390/ijms252011122.

[34] Ji W, Sun J, Hu Z, Sun B. Resveratrol protects against atherosclerosis by downregulating the PI3K/AKT/mTOR sig-

naling pathway in atherosclerosis model mice. Experimental and Therapeutic Medicine. 2022; 23: 414. https://doi.org/10.3892/etm.2022.11341.

[35] Wei J, Huang L, Li D, He J, Li Y, He F, *et al*. Total Flavonoids of Engelhardia roxburghiana Wall. Leaves Alleviated Foam Cells Formation through AKT/mTOR-Mediated Autophagy in the Progression of Atherosclerosis. Chemistry & Biodiversity. 2021; 18: e2100308. https://doi.org/10.1002/cbdv.202100308.

[36] Pi S, Mao L, Chen J, Shi H, Liu Y, Guo X, *et al*. The P2RY12 receptor promotes VSMC-derived foam cell formation by inhibiting autophagy in advanced atherosclerosis. Autophagy. 2021; 17: 980–1000. https://doi.org/10.1080/15548627.2020.1741202.

[37] Fan X, He Y, Wu G, Chen H, Cheng X, Zhan Y, *et al*. Sirt3 activates autophagy to prevent DOX-induced senescence by inactivating PI3K/AKT/mTOR pathway in A549 cells. Biochimica et Biophysica Acta. Molecular Cell Research. 2023; 1870: 119411. https://doi.org/10.1016/j.bbamcr.2022.119411.